Alternative Origin of Log-Normal Size Distributions of Crystallites in Controlled Solid-Phase Crystallization of Amorphous Si Thin Films

Hideya Kumomi*
R&D Headquarters, Canon Inc., 3-30-2 Shimomaruko, Ohta-ku, Tokyo 146-8501, Japan

Frank G. Shi
Department of Chemical and Biochemical Engineering and Materials Science, University of California, Irvine, California 92697-2575
(Received 12 October 1998)

Transmission-electron-microscopy observations reveal that the controlled solid-phase crystallization of amorphous Si thin films, which is exclusively initiated at the artificial nucleation sites, results in a log-normal size distribution of crystallites. The experimental observations can be fully described by a nucleation and growth theory developed by considering the interaction between the dynamics of nucleation and growth and that of the nucleation site depletion. Contrary to prevalent views, the formation of log-normal size distributions in phase transformations thus can be a consequence of the interplay between the dynamics of nucleation and growth and that of the nucleation site depletion, without involving any coarsening process. [S0031-9007(99)08773-6]

PACS numbers: 64.60.Qb, 64.70.Kb, 81.10.Jt, 81.30.Hd

Polycrystalline thin films are essential for advanced applications to the modern electric, optic, and magnetic devices such as Si-based thin-film transistors, solar energy converters, and magnetic recording media. Critical to the success of such applications is that the dimension of the crystallites and their size distribution be well controlled [1–5]. This is especially true of the minority-carrier devices with the highly recombination-active grain boundaries between the crystallites.

Solid-phase crystallization of amorphous thin films is one of the effective methods to obtain highly tailored polycrystalline thin films. However, a fundamental understanding of the amorphous-to-crystalline transformation is still far from complete. Particularly, the dynamic evolution of the crystallite-size distribution (CSD) during the phase transformation has been under investigation. In the early stages of the nucleation and growth, the dynamic evolution of the CSD exhibits a universal power-law behavior [6], which has been experimentally observed in the solid-phase crystallization of amorphous Si (a-Si) thin films [7]. The universal power-law behavior is valid before the depletion of the nucleation sites becomes significant. The intrinsic depletion of the nucleation sites during the nucleation and growth leads naturally to a nonlinear effect in the subsequent evolution of the CSD. Although it was suggested that the interplay between the dynamics of nucleation and growth could give rise to a log-normal CSD [8,9], no definite experimental evidence has been obtained excluding involvement of coarsening of the crystallites in the formation process.

The purpose of this Letter is to demonstrate both experimentally and theoretically that, contrary to prevalent views, the formation of log-normal CSDs in phase transformations can be a consequence of the interplay between the dynamics of nucleation and growth and that of the nucleation site depletion, without involving any coarsening process. This is accomplished by inducing the nucleation and growth of Si crystallites at artificially created nucleation sites in a-Si thin films. Only a single crystallite nucleates and subsequently grows at each artificial site; the sites are periodically placed in planes of the films. All of the nucleated crystallites continue to grow by incorporating Si atoms from the remaining a-Si phase, without the shrinkage and disappearance associated with the coarsening process, which is the classical origin of log-normal CSDs [10,11]. In addition, this novel experiment allows us to easily exclude coalescence of the crystallites. The observed log-normal CSD and its dynamic evolution are fully consistent with a nucleation and growth theory also presented herein. Thus our results reveal an alternative origin of log-normal CSDs which can often be observed in many technologically significant phase transformations.

The controlled solid-phase crystallization of a-Si thin films with the artificial nucleation sites was executed as follows [12]. 100-nm-thick a-Si films were first deposited over SiO_2-coated Si wafers at a temperature of 823 K, at a deposition rate of 2.8×10^{-2} nm s^{-1}, by low-pressure chemical-vapor deposition using silane gas under a pressure of 40 Pa. Si^+ ions were uniformly implanted into the films at an accelerating energy of 70 keV and at a dose of 4×10^{12} mm^{-2}. Then the Si^+ ions were implanted again at the same energy but at a higher dose of 2×10^{13} mm^{-2}, locally into the films except for small masked areas. The small masked areas are circular in radius of 0.33 μm and placed at the square lattice points in periods of 3 μm. Finally, the films were isothermally annealed in nitrogen atmosphere at a temperature of 873 K for some periods during which the small circular areas served as the artificial nucleation sites.

Transmission electron microscope (TEM) micrographs in Fig. 1 are the bright-field plan-view images of the annealed films, which show the evolution of the controlled crystallization with the annealing time. Each micrograph covers the area including four of the artificial nucleation sites which are visible as dark circular areas at the square lattice points. It is seen at 2.0×10^4 s [Fig. 1(a)] that a single dendritic crystallite grows from within each artificial site. The crystallites grow beyond the sites' areas at 3.6×10^4 s [Fig. 1(b)], and they are about to impinge upon the neighbors at 5.4×10^4 s [Fig. 1(c)]. These crystallites are found to be multiply twinned but contain the continuous crystalline structures, which indicates that they grow from the single nuclei. It is noted that no coalescence has occurred at least up to 5.4×10^4 s.

Figure 2 shows the dynamic evolution of the CSD which was observed from the samples shown in Fig. 1. The CSDs are represented by the number concentration of the crystallites, $f(r)$, as a function of the effective radius, r ($\equiv \sqrt{a_p/\pi}$), where a_p is the area of the dendritic crystallite projected onto the film. The plots indicated by three types of the discrete markers correspond to the CSDs at the three annealing times, respectively. It is seen that the log-normal CSD shifts toward the larger size with time preserving its log-normal form, but slightly broadens reducing its peak height. This observation evidently suggests that the log-normal CSD can arise without coarsening of the crystallites. The solid lines in Fig. 2 are the theoretical predictions from a nucleation and growth theory outlined in the following paragraphs.

The dynamic evolution of the CSD beyond the nucleation critical region is generally described by [6,7,13]

$$f(g,t) = \phi(g,t)\,\frac{\psi(g,t) - \psi(g,0)}{\psi(g,\infty) - \psi(g,0)}\,, \tag{1a}$$

$$\phi(g,t) = \frac{n(g,t)}{\sqrt{\pi}}\exp\!\left(-\frac{W_*}{kT}\right)\frac{\beta(g_*)}{\beta(g)}\,, \tag{1b}$$

$$\psi(g,t) = \mathrm{erfc}\left\{1 + \exp\left[\frac{\lambda\tau - t + t_g(g)}{\tau}\right]\right\}, \tag{1c}$$

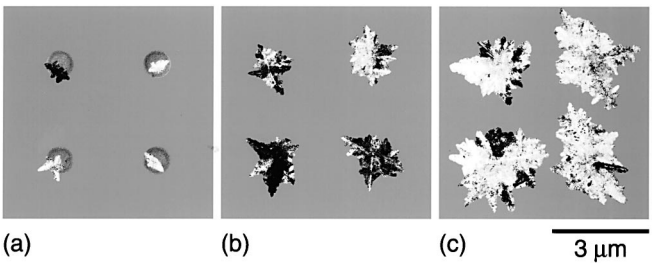

FIG. 1. Bright-field plan-view TEM images of a-Si thin films annelated at 873 K in nitrogen with the artificial nucleation sites, which show the evolution with the annealing time at (a) 2.0×10^4 s, (b) 3.6×10^4 s, and (c) 5.4×10^4 s. It is seen that a single dendritic crystallite grows at each artificial site, and no coalescence has occurred up to 5.4×10^4 s.

where $f(g,t)$ is the number concentration of crystallites composed of g monomers at a time t, $\phi(g,t)$ is the steady-state CSD, and $\psi(g,t)$ is the dynamic factor. In Eq. (1b), $n(g,t)$ is the density of the nucleation sites available at the time when g-sized crystallites at t had nucleated, W_* is the free-energy barrier to nucleation, k denotes Boltzmann constant, T represents the crystallization temperature, $\beta(g)$ is the addition rate of monomers into g-sized crystallites, and g_* is the critical size for nucleation. In Eq. (1c), τ is the period for a near-critical crystallite to pass diffusing across the critical region, $\lambda\tau$ is the time to establish the steady state in the subcritical region, and $t_g(g)$ is the time for a stable crystallite to grow from the right boundary of the critical region to g. The dynamic evolution of the CSD specific to the present experimental system can be obtained by giving the size (and time) dependence of $\beta(g)$, $t_g(g)$, and $n(g,t)$ as below.

In the solid-phase crystallization of amorphous materials, the addition of monomers into crystallites is determined by the chemical reaction at the interface between the crystallites and the amorphous matrices. The addition rates of monomers appearing in Eq. (1b) should be proportional to the surface area of the crystallites as

$$\beta(g) = \omega S(g)\,, \tag{2}$$

where ω is the rate of the monomer addition into the crystallites per unit area of their surface, and $S(g)$ is the surface area of g-sized crystallites. For the present experimental system using the amorphous thin films, the crystallites smaller than the film thickness can grow three dimensionally, but after reaching the film surface, the growth is restricted in the horizontal directions. Considering the general scaling geometry [7,13], the

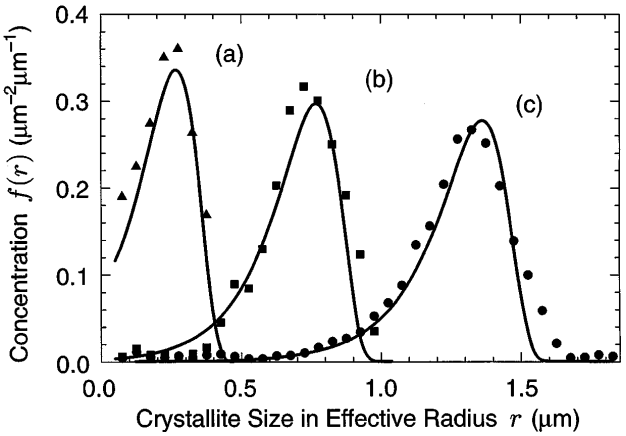

FIG. 2. Dynamic evolution of the CSD in the controlled solid-phase crystallization of a-Si thin films with artificial nucleation sites. Three CSDs marked with ▲, ■, and ● are observed in the samples shown by (a), (b), and (c) of Fig. 1, respectively. The solid lines are the theoretical predictions with the depletion of the nucleation sites taken into account.

surface area of these crystallites is described by

$$S(g) = \begin{cases} a_3 g^{1-1/d}, & g < g_\ell, \\ a_2 g^{1-3/2d}, & g \geq g_\ell, \end{cases} \tag{3}$$

where $a_3 = (36\pi v_1^2)^{1/3}$ and $a_2 = 2(\pi v_1 \ell)^{1/2}$, with v_1 and ℓ being the volume of a monomer and the film thickness, respectively, d is the effective dimension controlling the geometry of the crystallites, g_ℓ is the size at which the three dimensionally growing crystallites reach the film surfaces. Using the expression given above for $\beta(g)$, $t_g(g)$ [$\equiv \int^g dg'/\beta(g')$] in Eq. (1c) is thus given by

$$t_g(g) = \begin{cases} \dfrac{d}{\omega a_3} g^{1/d}, & g < g_\ell, \\ \dfrac{d}{\omega}\left[\dfrac{g_\ell^{1/d}}{a_3} + \dfrac{2(g^{3/2d} - g_\ell^{3/2d})}{3a_2} \right], & g \geq g_\ell. \end{cases} \tag{4}$$

On the other hand, the density of the nucleation sites available at the time when g-sized crystallites at t had nucleated is given by

$$n(g,t) = a_s n_0 n_s[t - t_g(g)], \tag{5}$$

where a_s is the area of an artificial nucleation site, n_0 is the initial density of the nucleation sites within the artificial site's area, and $n_s(t)$ is the density of the artificial sites having no crystallite at t. It is the most distinctive feature of the present system that only a single crystallite nucleates at each artificial nucleation site. The artificial sites available to the subsequent nucleation are being depleted one by one as a new crystallite nucleates. Therefore, $n_s(t)$ decreases with time and is determined by the formation rate of the crystallites as

$$\frac{dn_s(t)}{dt} + a_s n_s(t) \frac{dn_a(t)}{dt} = 0,$$

where

$$n_a(t) = \frac{\tau \omega a_3 n_0}{\sqrt{\pi}} \exp\left(-\frac{W_*}{kT}\right) \times \left[E_1(\epsilon e^{-t/\tau}) - E_1(\epsilon) - \frac{t}{\tau e^\epsilon} \right], \tag{6}$$

is the accumulated number concentration of the stable crystallites which have grown beyond the critical region, with $\epsilon = 2e^\lambda$ [6,14]. Under the initial conditions of $n_s(0) = n_s^0$ (the density of the placed artificial sites), $n_s'(0) = 0$, and $n_s(t) \to 0$, $n_s'(t) \to 0$ as $t \to \infty$, the above differential equation is solved to yield

$$n_s(t) = n_s^0 \exp[-a_s n_a(t)]. \tag{7}$$

Thus the CSD and its dynamic evolution in the controlled solid-phase crystallization of a-Si thin films with the artificial nucleation sites are analytically described by Eqs. (1)–(7) considering the interaction between the dynamics of nucleation and growth and that of the nucleation site depletion. These equations are transformed into the size space of the effective radius of the crystallites through the relation of $f(r,t)dr = f(g,t)dg$ with $r \equiv (3v_1 g/4\pi)^{1/3}$ for $g < g_\ell$, or $r \equiv (v_1 g/\pi\ell)^{1/2}$ for $g \geq g_\ell$.

The theoretical predictions indicated by the solid lines in Fig. 2 are obtained from the above theory with the parameters predetermined as follows. The effective dimension of the dendritic crystallites in Eqs. (3) and (4) is determined to be $d = 3.41$ by observing the correlation between the size and the perimeter of the crystallites sampled for the CSD [7]. The value for n_0 in Eqs. (5) and (6) is taken to be the atomic density of a-Si. The other nucleation and growth parameters included in Eqs. (1), (2), (4), and (6) cannot be arbitrarily chosen either. Fortunately, they are all available from the previous works in which their values were determined to be $W_* = 2.05$ eV, $\tau = 2.51 \times 10^3$ s, $\lambda = 1.20$, and $\omega = 4.17 \times 10^5\ \mu\text{m}^{-2}\,\text{s}^{-1}$ by the nucleation experiments using a-Si thin films without the artificial nucleation sites [7,13].

As demonstrated in Fig. 2, our simple theory reproduces the experimental results remarkably well, particularly the broadening of the CSD and the reduction of the peak height with time. It is noted that, if the crystallites are compact (i.e., $d = 3$), the CSD should simply shift with time, keeping its shape unchanged. Thus, the observed log-normal CSD, formed without coarsening of the crystallites, and its dynamic evolution are explained by the present nucleation and growth theory. This ascertains the depletion of the nucleation sites to be an alternative nonclassical origin of the log-normal CSD.

In the case of the classical origin invoking coarsening processes, the CSD becomes log-normal only at the long time limit when the transformed volume fraction is significant and the distance between the crystallites gets smaller so that they can interact or coalesce. However, our new mechanism suggests that the CSD can be log-normal from the early stages of phase transformations as soon as the finite nucleation sites have been depleted. In fact, as shown in Fig. 2, the CSD is already log-normal at 2.0×10^4 s although the crystallized volume fraction of the sample is less than 2%. It is likely that the CSD has already been log-normal due to the depletion of the nucleation sites long before the coarsening starts.

Figure 3 shows the log-log plot of the CSDs, in which the thick solid lines are the same log-normal CSDs as those in Fig. 2. The thin solid lines are the corresponding CSDs estimated from the present theory providing the nucleation sites were not depleted, and the dotted line presents their steady-state asymptotic limits. It is evident that the observed log-normal CSDs deviate from the corresponding CSDs without the depletion of the nucleation sites in their transient regions and never attain the steady state. This observation suggests that it is important to consider the depletion of the nucleation sites for the physics of nucleation and growth in general [15].

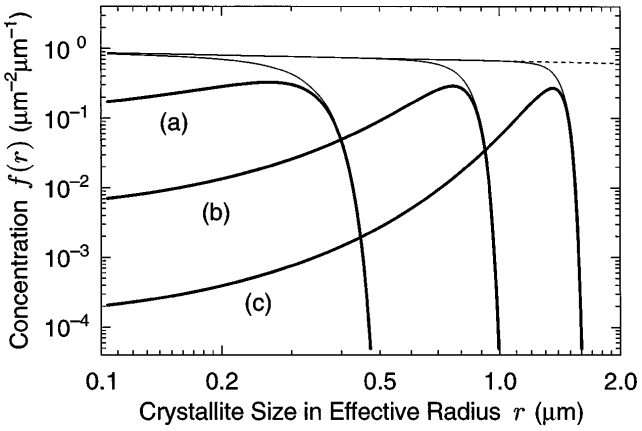

FIG. 3. Log-log plots of the log-normal CSDs formed with the artificial nucleation sites [thick solid lines; the same as those indicated by (a), (b), and (c) in Fig. 2], the corresponding CSDs estimated from the present theory providing the nucleation sites were not depleted (thin solid lines), and their steady-state asymptotic limits (dotted line).

In conclusion, TEM observations reveal that the controlled solid-phase crystallization of a-Si thin films, which is exclusively initiated at the artificial nucleation sites, results in a log-normal CSD without coarsening of the crystallites. The observed log-normal CSD shifts and slightly broadens with time reducing its peak height. These experimental observations can be fully described by a nucleation and growth theory developed that considers the interaction between the dynamics of nucleation and growth and that of nucleation site depletion. Thus it is demonstrated both experimentally and theoretically that, contrary to prevalent views, the formation of log-normal CSDs in phase transformations can be a consequence of the interplay between the dynamics of nucleation and growth and that of the nucleation site depletion, without involving any coarsening process.

We thank Toru Takahashi for encouraging us to accomplish this work.

*Electronic address: kumomi@gcds.canon.co.jp

[1] For a review, see N. Yamauchi and R. Reif, J. Appl. Phys. **75**, 3235 (1994).
[2] For a recent review, see R. B. Bergmann, J. Köhler, R. Dassow, C. Zaczek, and J. H. Werner, Phys. Status Solidi (a) **166**, 587 (1998).
[3] T. Min and J.-G. Zhu, J. Appl. Phys. **73**, 5548 (1993).
[4] C. Yang, J. M. Sivertsen, and J. H. Judy, IEEE Trans. Magn. **34**, Part I, 1606 (1998).
[5] Y. Nakatani, N. Hayashi, Y. Uesaka, and H. Fukushima, IEEE Trans. Magn. **34**, Part I, 1618 (1998).
[6] F. G. Shi and J. H. Seinfeld, Mater. Chem. Phys. **37**, 1 (1994).
[7] H. Kumomi and F. G. Shi, Phys. Rev. B **52**, 16 753 (1995).
[8] R. B. Bergmann, F. G. Shi, and J. Krinke, Phys. Rev. Lett. **80**, 1011 (1998).
[9] R. B. Bergmann, F. G. Shi, H. J. Queisser, and J. Krinke, Appl. Surf. Sci. **132**, 376 (1998).
[10] I. M. Lifshitz and V. V. Slyozov, J. Phys. Chem. Solids **19**, 35 (1961).
[11] C. Wagner, Z. Elektrochem. **65**, 581 (1961).
[12] H. Kumomi, T. Yonehara, and T. Noma, Appl. Phys. Lett. **59**, 3565 (1991).
[13] H. Kumomi and F. G. Shi, Mater. Res. Soc. Symp. Proc. **472**, 403 (1997).
[14] G. Shi and J. H. Seinfeld, J. Mater. Res. **10**, 2091 (1991).
[15] Z. Kožíšek, P. Demo, and M. Nesladek, J. Chem. Phys. **108**, 9835 (1998).